FINAL REPORT

Electrochemical Oxidation of Perfluoroalkyl Acids in Still Bottoms from Regeneration of Ion Exchange Resins

SERDP Project ER18-1320

MARCH 2021

Qingguo Huang
University of Georgia

Steve Woodard
Michael Nickelsen
ECT2

Dora Chiang
CDM Smith

Shangtao Liang
Rebecca Mora
AECOM

Distribution Statement A
This document has been cleared for public release

SERDP
DOD ▪ EPA ▪ DOE

This report was prepared under contract to the Department of Defense Strategic Environmental Research and Development Program (SERDP). The publication of this report does not indicate endorsement by the Department of Defense, nor should the contents be construed as reflecting the official policy or position of the Department of Defense. Reference herein to any specific commercial product, process, or service by trade name, trademark, manufacturer, or otherwise, does not necessarily constitute or imply its endorsement, recommendation, or favoring by the Department of Defense.

REPORT DOCUMENTATION PAGE

Form Approved
OMB No. 0704-0188

Public reporting burden for this collection of information is estimated to average 1 hour per response, including the time for reviewing instructions, searching existing data sources, gathering and maintaining the data needed, and completing and reviewing this collection of information. Send comments regarding this burden estimate or any other aspect of this collection of information, including suggestions for reducing this burden to Department of Defense, Washington Headquarters Services, Directorate for Information Operations and Reports (0704-0188), 1215 Jefferson Davis Highway, Suite 1204, Arlington, VA 22202-4302. Respondents should be aware that notwithstanding any other provision of law, no person shall be subject to any penalty for failing to comply with a collection of information if it does not display a currently valid OMB control number. **PLEASE DO NOT RETURN YOUR FORM TO THE ABOVE ADDRESS.**

1. REPORT DATE *(DD-MM-YYYY)*	2. REPORT TYPE	3. DATES COVERED *(From - To)*
02-03-2021	SERDP Final Report	7/16/2018 – 7/15/2021

4. TITLE AND SUBTITLE
Electrochemical Oxidation of Perfluoroalkyl Acids in Still Bottoms from Regeneration of Ion Exchange Resins

5a. CONTRACT NUMBER
W912HQ18C0016

5b. GRANT NUMBER

5c. PROGRAM ELEMENT NUMBER

6. AUTHOR(S)
Huang, Qingguo; Woodard, Steven; Nickelsen, Michael; Chiang, Mora, Rebecca

5d. PROJECT NUMBER
ER18-1320

5e. TASK NUMBER

5f. WORK UNIT NUMBER

7. PERFORMING ORGANIZATION NAME(S) AND ADDRESS(ES)
The University of Georgia
1109 Experiment St.
Griffin, GA 30223

8. PERFORMING ORGANIZATION REPORT NUMBER
ER18-1320

9. SPONSORING / MONITORING AGENCY NAME(S) AND ADDRESS(ES)
SERDP PROGRAM OFFICE
PROGRAM MANAGER
4800 MARK CENTER DRIVE, SUITE 16F16
ALEXANDRIA VA 22350-3600

10. SPONSOR/MONITOR'S ACRONYM(S)
SERDP

11. SPONSOR/MONITOR'S REPORT NUMBER(S)
ER18-1320

12. DISTRIBUTION / AVAILABILITY STATEMENT

Distribution A: Approved for public release; distribution is unlimited.

13. SUPPLEMENTARY NOTES

14. ABSTRACT
Still bottoms are wastes produced from regeneration of saturated ion exchange resin (IXR) by a solution containing high salt content and methanol followed by distillation to remove the methanol. Still bottoms contain high concentrations of per- and polyfluoroalkyl substances (PFASs), and thus their disposal can be a factor limiting the widespread application of IXR technology on PFAS contaminated sites. This study investigated the treatment of perfluoroalkyl acids (PFAAs) in still bottoms during electrochemical oxidation (EO) using Magnéli phase titanium suboxide (Ti_4O_7) as the anode. The results demonstrate the promise of coupling regenerable IXR technology and EO for removing PFAAs from water and destroying them onsite.

15. SUBJECT TERMS
Electrooxidation, Ion Exchange Resins, PFAAs, Still Bottoms, Perchlorate, Groundwater

16. SECURITY CLASSIFICATION OF:			17. LIMITATION OF ABSTRACT	18. NUMBER OF PAGES	19a. NAME OF RESPONSIBLE PERSON
a. REPORT	b. ABSTRACT	c. THIS PAGE			Qingguo Huang
U	U	U	SAR	38	19b. TELEPHONE NUMBER *(include area code)* 770-229-3302

Table of Content

ABSTRACT:

Introduction and Objectives

Still bottoms are wastes produced from regeneration of saturated ion exchange resin (IXR) by a solution containing high salt content and methanol followed by distillation to remove the methanol. Still bottoms contain high concentrations of per- and polyfluoroalkyl substances (PFASs), and thus their disposal can be a factor limiting the widespread application of IXR technology on PFAS contaminated sites. The goal of this study was to investigate the treatment of perfluoroalkyl acids (PFAAs) in still bottoms during electrochemical oxidation using Magnéli phase titanium suboxide (Ti_4O_7) as the anode.

Technical Approach

This study examined the feasibility of using Ti_4O_7-based EO to remove PFASs from still bottoms recovered from regenerated IXR media. The still bottoms were generated by a unique solvent/non-chloride brine regeneration of PFASs loaded IXR resin. Various solvent/salt regenerant solutions were evaluated. The efficiency of IXR regeneration solutions was compared in terms of PFAS elution. The fate of Cl^- was monitored and factors impacting the formation of ClO_3^- and ClO_4^- during EO treatment were assessed.

Results

All 10 monitored PFAAs were effectively degraded by electrochemical oxidation (EO) on a Magnéli phase Ti_4O_7 anode, and the removal was 61.1% after 40-h EO treatment of a still bottoms sample that was produced from the use of a typical regenerant containing 2% NaCl and 80% methanol by mass. Total Organic Carbon (TOC) destruction exceeded 79% in this treatment. Chlorate (ClO_3^-) and perchlorate (ClO_4^-) were formed after 8 h and reached a maximum of 2.3 mM and 2.2 mM, respectively, after 40 h. To minimize perchlorate generation by EO, five other salts were also tested instead of NaCl to regenerate IXR that had treated groundwater containing PFAAs. The regenerant containing NaI exhibited the greatest PFAAs elution, comparable to that of NaCl. EO treatment of the still bottoms produced from the NaI regenerant for 200 h led to a total of 98.1% removal of all 10 monitored PFAAs. No ClO_3^- or ClO_4^- was detected after 100 h of EO treatment. It was found that the methanol residue in still bottoms effectively suppressed the formation of ClO_3^- and ClO_4^- during electrooxidation by scavenging chlorine radicals. Persulfate pretreatment did not appear to enhance PFAA degradation during EO treatment.

Benefits

The results of this study demonstrate the promise of coupling regenerable IXR technology and EO for removing PFAAs from water and destroying them onsite.

Keywords

Electrooxidation, PFAAs, Still Bottoms, Perchlorate, Groundwater

1. Introduction

Per- and polyfluoroalkyl substances (PFASs) have been used extensively in industrial, medical, and commercial applications since the 1950s [1-4]. PFASs have recently been subjected to increasingly intensive research, because they are highly persistent, bio-accumulative and have been found toxic. Some PFASs, perfluorinated sulfonic and carboxylic acids in particular, are extremely resistant to degradation and have therefore been detected ubiquitously in the environment, biota, food items, and humans [5-9]. Perfluorooctanesulfonate (PFOS) and perfluorooctanoic acid (PFOA) are the two most commonly used perfluoroalkyl acids (PFAAs) [10-12].

Destruction of PFAAs is difficult because of their intrinsic persistence [13, 14]. Separation technologies, such as granular activated carbon (GAC), ion exchange resin (IXR) exchange/adsorption, nanofiltration (NF) and reverse osmosis filtration, have been shown effective for removing PFASs from water [15-20], and are currently used to manage PFAS-contaminated drinking water. Ion exchange resin (IXR) exchange/adsorption can efficiently remove both short and long chain PFAAs[21]. Some IXR can be regenerated on-site [22]. Regeneration of IXR results in reusable IXR for PFASs removal, eliminating the disposal or incineration of spent IXR, and the regenerant wastewater containing desorbed PFASs. The regenerant wastewater can be distilled to reclaim methanol vital for IXR regeneration process. The post-distillation process generates a low-volume, high-concentration liquid waste known as still bottoms which contain high concentrations of PFASs, salts, and residual organic content. Therefore, this IXR adsorption and regeneration process transfers PFASs from a very large volume of contaminated water to a highly concentrated small volume of still bottoms, making subsequent disposal or destruction much more manageable. It should be noted that IXR regeneration is not operated continuously and is needed only when the regenerable IXR is spent. The frequency of regeneration varies by several factors and is highly site specific, typically ranging from 1 to 3 months based on the research team's operation experience. The still bottoms containing concentrated PFASs are transferred to a different synthetic adsorbent/IXR for subsequent disposal, a process referred to as "super loading".

It is desirable to have alternative technologies capable of destroying PFASs instead of off-site disposal of still bottoms. A number of studies have demonstrated that electrooxidation (EO) can mineralize PFAAs at room temperature and atmospheric pressure without additional reagents [7, 13, 23-28]. EO is a chemical destructive technology that promotes direct electron transfer from organic contaminants to the anode, thus converting them into free radicals, which can then be attacked by hydroxyl free radicals that are also generated on the anode surfaces during the EO process [1]. EO is a promising water/wastewater treatment technology for different uses, as it can be applied to a wide spectrum of pollutants at ambient conditions and is relatively energy efficient in comparison to other AOP technologies [14, 29-31]. However, due to its strong oxidation potential, EO can generate byproducts, such as chlorate and perchlorate, when chloride is present in the wastewater.

Magnéli phase titanium sub-oxides, such as Ti_4O_7, have recently been explored as promising electrode materials for EO applications because of their high conductivity and chemical inertness [32-34]. Ti_4O_7 is an ideal electrode for electrochemical

wastewater treatment because of its great conductivity, robustness in aggressive solutions [35-38] and a wide electrochemical window with respect to water decomposition (~1.20 V and 2.9 V vs. SHE) [36]. It has been shown that Ti_4O_7 is a typical "non-active" anode, producing hydroxyl free radicals ($HO^{\bullet}$) via water oxidation, and is also active for direct electron transfer reactions [36, 39]. Magnéli phase titanium suboxides have been used as anodes in electrochemical oxidation to degrade a number of organic chemicals, including substituted phenols [39, 40], trichloroethylene [41, 42], chloroform [42], tetracycline [43], and amoxicillin [33]. Our recent studies have demonstrated the degradation and mineralization of PFOS on Magnéli phase Ti_4O_7 electrode [1, 44-46].

Despite the advantage of EO involving Magnéli phase Ti_4O_7 anode, EO is not yet feasible to directly treat large volumes of groundwater containing low concentrations of PFASs. This is because the mass transfer of the target chemical from bulk solution to the anode surfaces is limited when its concentration is low, thus limiting the overall EO efficiency [47]. Increasing the PFASs concentrations in the solution is one way to overcome this rate limitation by interfacial mass transfer. Therefore, coupling the EO treatment using Magnéli phase Ti_4O_7 anode with another treatment procedure that concentrates PFASs prior to the EO procedure, such as regenerable IXR treatment, would be beneficial. In addition, the salt components in still bottoms provide the electrolytes needed for EO treatment, and thus EO may offer an option to potentially mineralize PFASs in high salt content waste streams.

Chloride (Cl^-) is a common anion in natural water, and may be converted into reactive chlorine species (e.g., free chlorine and chlorine radicals) on an anode and further oxidized to undesirable byproducts, such as chlorate (ClO_3^-) and perchlorate (ClO_4^-) [48-51], which can cause serious health risks to human and animals, including disruption of the normal function of the thyroid gland and carcinogenic potential [48, 51, 52]. The transformation of Cl^- during EO degradation of PFOS on Ti_4O_7 anode has been reported in our recent study [45], but the fate of Cl^- in highly organic/salty wastewater matrices remains unexplored.

This project examined the feasibility of using Ti_4O_7-based EO to remove PFASs from still bottoms recovered from regenerated IXR media. The still bottoms were generated by a unique solvent/non-chloride brine regeneration of PFASs loaded IXR resin [53]. Various solvent/salt regenerant solutions were evaluated. The efficiency of IXR regeneration solutions was compared in terms of PFAS elution. The fate of Cl^- was monitored and factors impacting the formation of ClO_3^- and ClO_4^- were assessed. We have also tested pretreatments of the still bottoms with persulfate to reduce organic contents prior to EO treatment in order to evaluate the effects of pretreatment on the performance of EO in removing PFAS in still bottoms. The results of the study provide a basis for coupling IXR and Ti_4O_7-based EO technologies for an integral solution of PFASs contaminated waters.

2. Materials and methods

2.1 Chemicals

All chemicals used in the experiments were reagent grade or higher and used as received. PFOS (98%) was provided by Indofine Chemical Company, Inc. (Somerville, NJ), chlorate (ClO_3^-) was from Sigma-Aldrich (St. Louis, MO). Sodium perfluoro-1-[^{13}C8]-octanesulfonate (M8PFOS) and other PFASs standards were obtained from Wellington Laboratories (Ontario, Canada). Perchlorate (ClO_4^-), sodium chloride (NaCl) and HPLC grade methanol (MeOH) were purchased from Fisher Chemical. Sodium sulfate (Na_2SO_4) was obtained from J.T. Baker. NaOH, Na_2CO_3, $NaHCO_3$ and NaI were from Sigma Aldrich. IXR resin, SORBIX A3F, was provided by ECT2. All solutions were prepared in ultrapure water (≥18.2 MΩ/cm at 20 °C) produced by a Barnstead Nanopure water purification system (Thermo Scientific, U.S.).

2.2 Regenerable IXR operation and generation of still bottoms samples

A typical regenerable IXR operation comprises the following steps (1) contaminated groundwater is pumped through the regenerable IXR vessel wherein PFASs compounds are adsorbed, (2) saturated ion exchange resin is regenerated by elution using a solvent/brine solution, (3) the "spent regenerant" is distilled to recover the solvent (typically, methanol) for reuse. The residual is a very highly concentrated PFASs / brine mixture, also known as still bottoms. NaCl is the most common salt used in the IXR regenerant. EO treatment of highly concentrated chloride ion solutions results in the formation of chlorate and perchlorate [50, 52]. Therefore, the use of different salts for IXR regeneration was also evaluated in this study.

A pilot-scale regenerable IXR fiberglass reinforced plastic vessel (23 cm diameter x 122 cm long) containing 34.6 L of resin was operated on a site with PFASs-contaminated groundwater for approximately 61,000 bed volumes, at which ~ 4% PFASs breakthrough was observed. The saturated resin was regenerated, and then PFASs were eluted in a bench scale column (2.5 cm diameter x 25 cm long) using 2 bed volumes (BV) of a 2% by weight salt solution in DI water at a flow rate of 1 BV/hr followed by 5 BV of a regenerant solution consisting of 80% by volume methanol (MeOH) and 2% by weight salt, at a flow rate of 1 BV/hr. In addition to NaCl, the following five other salts were tested: NaOH, Na_2CO_3, $NaHCO_3$, Na_2SO_4, and NaI. Of the six salts tested, MeOH/NaCl and MeOH/NaI regenerant solutions exhibited the highest eluted PFASs concentrations. Methanol from each spent regenerant solution was recovered by distillation, leaving behind still bottoms comprising ~10% by weight salt and elevated PFASs concentrations. The still bottoms derived from the distillation of the MeOH/NaCl spent regenerant solution are hereafter named Still Bottoms I, and similarly the MeOH/NaI still bottoms sample is hereafter named Still Bottoms II. The major properties of each still bottoms sample are listed in Table 1, and their PFASs contents are presented in Table A1 in Appendix. It should be noted that Still Bottoms I and II were generated from IXR operations at different times, and thus variation in the influent water may have contributed partially to their difference in properties shown in Table 1.

Table 1. Properties of the still bottom samples.

Property	Still Bottoms I	Still Bottoms II
pH	9.57 ± 0.3	9.64 ± 0.5
Conductivity ($mS \cdot cm^{-1}$)	15.89	25.15
TOC ($mg\ C \cdot L^{-1}$)[a]	13,280	201,529
$[Cl^-]$($mg \cdot L^{-1}$)	62,716	3,579
Methanol ($mg \cdot L^{-1}$)	124	216

[a] Total organic carbon.

2.3. EO procedures

Electrochemical oxidation was performed in an undivided electrolytic cell (10 cm × 5 cm × 2.5 cm) with a rectangular Ti_4O_7 ceramic plate (10 cm × 5 cm) as the anode. Information about fabrication and characterization of Ti_4O_7 is described in detail in Appendix (Text A1). Two 304 stainless steel plates of the same size were placed in parallel to the anode on either side at a 2.5 cm gap as cathodes. In each treatment, the electrolytic cell contained a 100 mL still bottom sample, stirred at 700 rpm, and operated under a constant current density, supplied by a controllable DC power source (Electro Industries Inc., Monticello, MN). The anode potential was monitored using an open circuit three electrode system with an Ag/AgCl reference electrode by a CHI 660E electrochemical workstation (CH Instruments, Inc., Austin, TX), and the potential drop in solution (iRs) was compensated. At pre-selected time intervals, the power source was paused with the solution continuously stirred to ensure homogeneity, and then triplicate samples, 0.5 mL each, were collected and stored at 4 °C for subsequent analysis. For the experiment with Still Bottoms II a new set of electrodes were replaced after 100 h of EO treatment. All experiments were conducted at least in duplicate and performed at room temperature. The solution temperature was monitored and found no obvious change during electrolysis. The pH was also measured during treatment using an ion selective electrode (Oakton pH 300 series).

2.4. Analytical methods

Each sample (0.5 mL) was mixed with 4.5 mL methanol and filtered through a 0.22 μM cellulose membrane. The concentrations of PFASs compounds (Table A2 for a full list) were analyzed using a Waters ACQUITY UPLC system coupled with Xevo TQD tandem mass spectrometry (UPLC-MS/MS) (Milford, MA) and quantified using calibrations with isotope-labeled internal standards, with more detail described in Appendix (Text A2).

TOC analyses were performed using a TOC-L total organic carbon analyzer (Shimadzu, Co. Ltd., Japan). The Cl^- and F^- in selected samples were analyzed with an anion chromatography system (Dionex, USA) equipped with a conductivity detector (ADRS 600, 2 mm, Dionex, USA), a high capacity hydroxide-selective ion chromatography analytical column (AS18, 2 × 250 mm, Thermo Fisher Scientific, USA), and a guard column (AG18, 2 × 50 mm, Thermo Fisher Scientific, USA). A KOH solution of 40 mM was used as the mobile phase at a flow rate of 0.25 mL/min. The detection limit for Cl^- and F^- was 0.005 μM.

Defluorination ratio (F_r) was calculated using the measured amount of released fluoride divided by the total fluorine contained in the PFASs that had been removed as indicated in the below equation (E1):

$$F_r = \frac{C_{F[t]} - C_{F[0]}}{\sum n_{F,i} \times (C_0 - C_t)_i} \quad \text{(E1)}$$

Where $C_{F[t]}$ and $C_{F[0]}$ are the concentrations of fluoride ion (μM) at time t and 0 respectively; C_0 and C_t are the concentrations of PFASs (μM) at time 0 and t respectively; and the factor *n* corresponds to the number of fluorine atoms in PFASs molecule.

For selected treatments, samples were also collected for determination of ClO_3^- and ClO_4^-, which were quantified using the Waters ACQUITY UPLC-MS/MS (Milford, MA). An ACQUITY UPLC BEH 1.7-micron C18 column (Waters, Milford, MA) was used for UPLC separation. The mobile phase consisted of 50% water (A) and 50% methanol (B) running at 0.3 mL/min. Electrospray ionization was operated in negative mode with the capillary voltage at 3 kV and the source temperature at 400 °C. ClO_3^- and ClO_4^- were quantified using multiple reactions monitoring (MRM) based on the transition m/z = 83 > 67 for ClO_3^-, and m/z = 99 > 83 for ClO_4^-. Quantification was achieved using a five-point calibration curve. The limit of quantification of ClO_3^- and ClO_4^- was 0.05 mg/L and 0.025 mg/L, respectively.

2.5 Persulfate treatment

An experiment was carried out to assess treatment of still bottoms I sample using thermally activated persulfate. To this end, 250 mL of the still bottoms sample was mixed with potassium persulfate at 0, 100, 150 or 200 mM and then incubated in water bath at 60° C for 24 hours. Samples were taken at different time intervals for Total Organic Carbon (TOC) analysis. Further, an additional experiment was performed to test the effect of persulfate pretreatment on the efficiency of EO treatment. To this end, still bottoms I sample was first treated by thermally activated persulfate as described above at 200 mM, and then the treated solution was subject to EO treatment as described in 2.3. Samples were taken at different times for PFAS analysis as described above.

3. Results and discussion

3.1. PFASs degradation in still bottoms I

As described in section 2.2, still bottoms I was prepared by elution of the PFASs-loaded IXR resin with a regenerant containing NaCl and MeOH followed by distillation to remove MeOH. This is a typical IXR regeneration process that is used in current field applications of IXR treatment for PFASs-contaminated groundwater. As seen in Fig. 1, the removal of selected PFASs after 40 h of EO treatment was evident, including PFOS, PFOA, perfluoro-1-hexanesulfonate (PFHxS), perfluoro-n-heptanoic acid (PFHpA), perfluoro-1-heptanesulfonate (PFHpS), reaching 98.9%, 94.8%, 95.0%, 56.9%, and, 96.8%, respectively (Table A1 in Appendix). The time course data of both PFOS and PFOA are displayed in Fig. 2, and those of the other PFAAs are shown in Fig. A1 (Appendix). No appreciable adsorption of PFASs on the Ti_4O_7 anode was observed (Fig. A2). Thus, the removal of PFASs was most likely attributed

to electrochemical reactions. Also seen in Fig. 2 and A1, the concentrations of short chain PFASs compounds were fairly stable during the 40 h EO treatment, such as perfluoro-1-butanesulfonate (PFBS) and perfluoro-1-pentanesulfonate (PFPeS), while the concentrations of perfluoro-n-butanoic acid (PFBA), perfluoro-n-pentanoic acid (PFPeA), and perfluoro-nhexanoic acid (PFHxA) increased, possibly from partial degradation of precursor compounds or longer-chain PFAAs[54]. The removal of the analyzed PFAAs was about 61.1% after 40 h of EO treatment, while a 79.5 % reduction of TOC was achieved during the same treatment duration. It should be noted that there were organic matters in the still bottoms sample other than those analyzed PFASs that could have also undergone destruction and mineralization during EO.

The surface area normalized pseudo-first order rate constants (k_{SA}) were calculated for PFASs exhibiting a high degree of degradation in still bottoms I, which are listed in Table A2 to compare with those obtained from our earlier research in mixture solution prepared by spiking PFASs in water [46]. The degradation of longer chain PFASs appeared to be faster than shorter chain ones. It should be noted that the measured k_{SA} in mixture solutions may be interfered with partial degradation of PFAA precursors, and thus this rate analysis can only be taken as qualitative, but the observed trend of faster degradation for the longer chain PFASs was also found in our earlier studies with solutions spiked with individual PFAS [46]. Furthermore, the degradation of perfluoroalkyl sulfonates (PFSAs) was faster than that of perfluoroalkyl carboxylic acids (PFCAs) under the experimental conditions, which is also consistent with previous work conducted with PFASs spiked water [46]. In addition, the k_{SA} values for PFASs degradation in still bottoms I was at least an order of magnitude lower than those in PFASs spiked in water. This difference may be attributed to the high concentrations of Cl^- as well as the organic matters in the still bottoms, which compete with PFASs for hydroxyl radicals generated on the anode surface during electrolysis.

The concentration of fluoride in the solution was also quantified at the end of treatment, and a defluorination ratio (F_r) was calculated via dividing the released F^- concentration by the total fluorine in the PFASs that have been removed from the solution by measurement. A fairly low defluorination ratio (5.1%) was detected. It differs from the result obtained for a solution prepared by spiking PFAAs in pure water in our previous study [46], in which the defluorination ratios after 8 h treatment were consistently above 90% when the current density was above 10 $mA \cdot cm^{-2}$. The low fluoride concentration detected in the still bottoms may partly result from the matrix effect that hindered fluoride detection. We have later improved the protocol used for fluoride analysis and obtained a better recovery, which will be discussed in 3.7. A recent study did observe a measurable adverse impact of NaCl on the defluorination of PFAS during EO [55].

During the EO treatment, the original dark brown color of the sample faded over time and eventually became clear (Fig. A3a). The pH value of the still bottoms was slightly reduced after 40 h treatment (from 9.57 to 9.26), while the TOC removal was about 79.5% when the current density was at 10 $mA \cdot cm^{-2}$. The color change of the still bottoms may result from a combination of TOC removal and the pH change of the solution by electrooxidation.

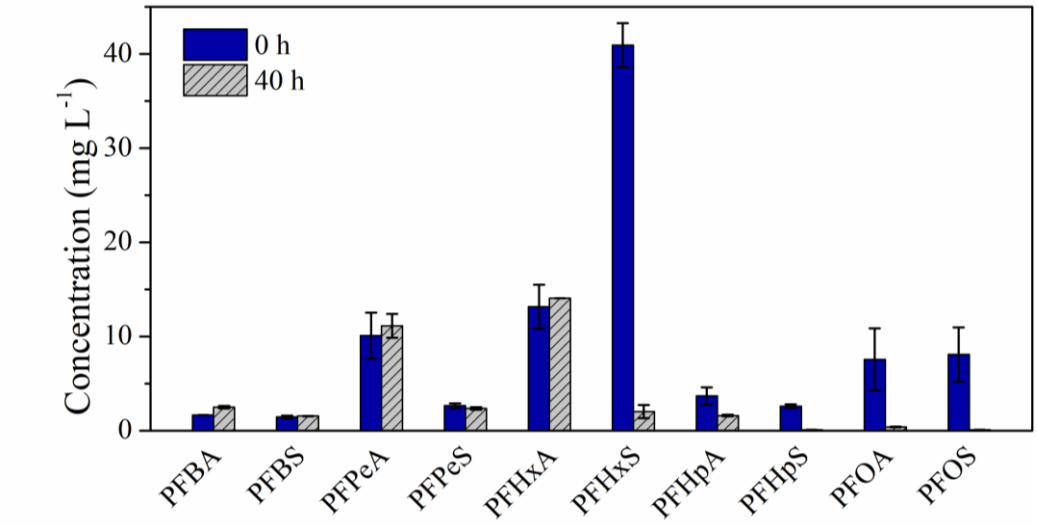

Fig. 1 Degradation of 10 PFAAs in Still Bottoms I on electrochemical oxidation treatment on Ti_4O_7 electrode. Current density = 10 mA·cm^{-2}, reaction time = 40 h. Error bars mean standard deviation of replicates.

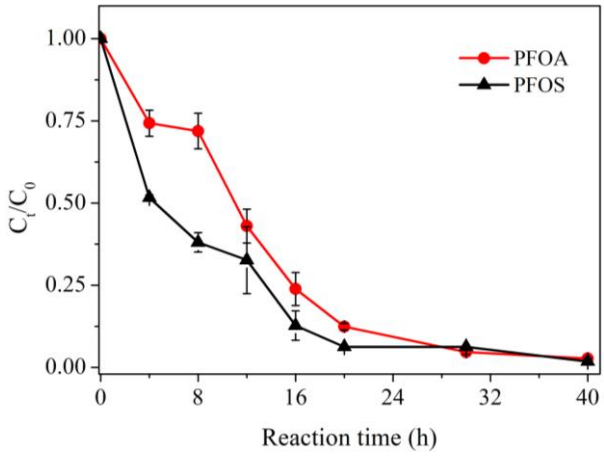

Fig. 2 Degradation of PFOA and PFOS in still bottoms sample I during electrochemical oxidation treatment on Ti_4O_7 electrode. Current density = 10 mA·cm^{-2}, reaction time = 40 h. Error bars mean standard deviation of replicates.

3.2. ClO_3^- and ClO_4^- formation during still bottom electrolysis.

Generally, Cl^- can be transformed to ClO_3^- and ClO_4^- in electrooxidation systems. Fig. 3 shows the formation of ClO_3^- and ClO_4^- during degradation of PFASs in still bottoms sample I on Ti_4O_7 anodes. No appreciable ClO_3^- and ClO_4^- was formed during the first 8 h of the treatment, and then their concentrations increased continuously. As shown in Fig. 3, ClO_3^- and ClO_4^- reached 2.3 mM and 2.2 mM, respectively, in 40 h, which combined accounts for about 0.27% of the total chloride initially included in the solution. It was shown in our previous study [45] that ClO_3^- and ClO_4^- were formed during EO treatment of PFOS spiked solution in the presence of 1 mM Cl^- with Ti_4O_7 anode, while the formation of ClO_3^- and ClO_4^- started as soon as the EO began and their combined formation accounted for 97.9% of added chloride

after 30 h of electrolysis. However, in this study no appreciable ClO_3^- and ClO_4 was formed for the first 8 h during EO treatment of still bottoms I. Previous studies have shown that high levels of dissolved organic carbon scavenged the chlorine produced from chloride oxidation and, thus, limited perchlorate formation when using electrooxidation to treat landfill leachates with a BDD anode [56], in which chlorate formation was delayed, while perchlorate was not detected during EO in the presence of high Cl^- content. The high organic matter content in still bottoms I may also have played a similar role in this study. In particular, methanol is an organic component that is used in IXR regenerant, and a small fraction remains in the still bottoms after methanol recovery via distillation, as shown in Table 1. Our study (described below) indicated that methanol minimizes the formation of ClO_3^- and ClO_4^- during electrooxidation.

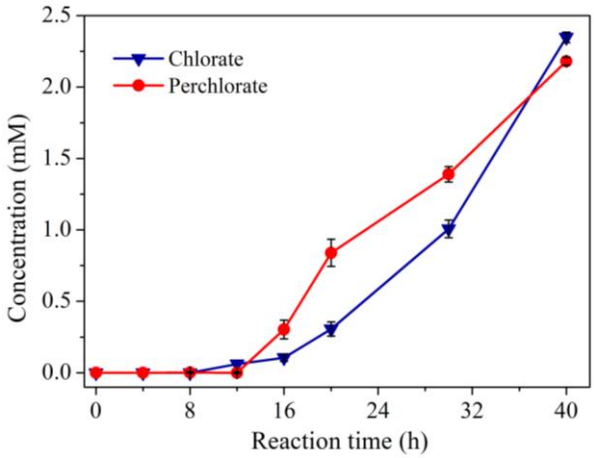

Fig. 3 Formation of ClO_3^- and ClO_4^- during the oxidation of PFASs in still bottom sample I. Current density = 10 mA·cm^{-2}. Error bars mean standard deviation of replicates.

3.3 Effects of methanol on formation of ClO_3^- and ClO_4^- and PFOS degradation

In order to evaluate the impact of methanol on the formation of ClO_3^- and ClO_4^- during EO process, an EO experiment was performed with Ti_4O_7 anode in prepared solutions containing 1.0 mM Cl^-, varying quantities of methanol and 100 mM Na_2SO_4. The solution containing methanol at different quantities had slightly different conductivities. Specifically, the conductivity was 15.89 mS cm^{-1} in the absence of methanol, while it decreased to 13.98 mS cm^{-1} when methanol was at 1000 mM. However, the anodic potential was relatively constant at the same current density (10 mA·cm^2) with methanol at different levels (Fig. A4). Thus, the effects of methanol on ClO_3^- and ClO_4^- formation could be observed at similar anodic potentials when the same current density was applied as in this study. Fig. 4a shows that ClO_3^- reached its temporal maximum of 382.0 μM in the first 4 h and then decreased in the absence of methanol at the current density of 10 mA·cm^{-2}. The value decreased to 77.5 and 0.0 μM when 20 mM and 100 mM methanol were spiked, respectively. ClO_4^- concentration increased and reached approximately 629.0 μM in 8 h in the absence of methanol (Fig. 4b). The values decreased to 302.9 and 32.3 μM when the methanol was increased respectively to 20 and 100 mM, and a further increase of methanol to 1000 mM led to no ClO_4^- formation during 8 h treatment. These indicate that methanol inhibited the formation of ClO_3^- and ClO_4^-.

It has been proposed that ClO_4^- is formed via a multistep pathway (R1 and R2), starting with the oxidation of Cl^- to form $Cl^•$ by direct electron transfer (DET) on BDD anode [48, 57]. Our

previous studies proved that DET of Cl^- did not occur on the Ti_4O_7 anode, on which $Cl^•$ was primarily formed via indirect routes (R3 and R4). $Cl^•$ can react immediately with Cl^- yielding $Cl_2^{•-}$ or couple to each other to form free chlorine (Cl_2/HOCl) (R5, R6, and R7). Chlorine radical species (CRS) are less reactive than the hydroxyl free radicals that are formed and bound on the anode surface ($HO^•_{ads}$), thus allowing for their accumulation and diffusion away from the anode surface. Therefore, methanol, although not reaching the anode surface [45], can still scavenge $Cl^•$ in the bulk solution, leading to reduced ClO_3^- and ClO_4^- formation when methanol is present in solution. The reaction rate constant between methanol and $Cl^•$ is 5.7×10^9 M^{-1} s^{-1} [58], similar to that of the reaction between $Cl^•$ and Cl^- yielding $Cl_2^{•-}$ (6.5×10^9 $M^{-1}\cdot s^{-1}$).

It should be noted from the data shown in Fig. A5 that approximately 99.9% of the PFOS was degraded in 20 min during EO in the absence of MeOH at the current density of 10 $mA\cdot cm^{-2}$, and no effect on degradation of PFOS was seen in the presence of 1 M MeOH. This is because methanol may have degraded before reaching the anode surface, and thus can only quench hydroxyl radicals in bulk solution [45, 59], but not those on the anode surface ($HO^•_{ads}$) that are responsible for PFASs degradation [45].

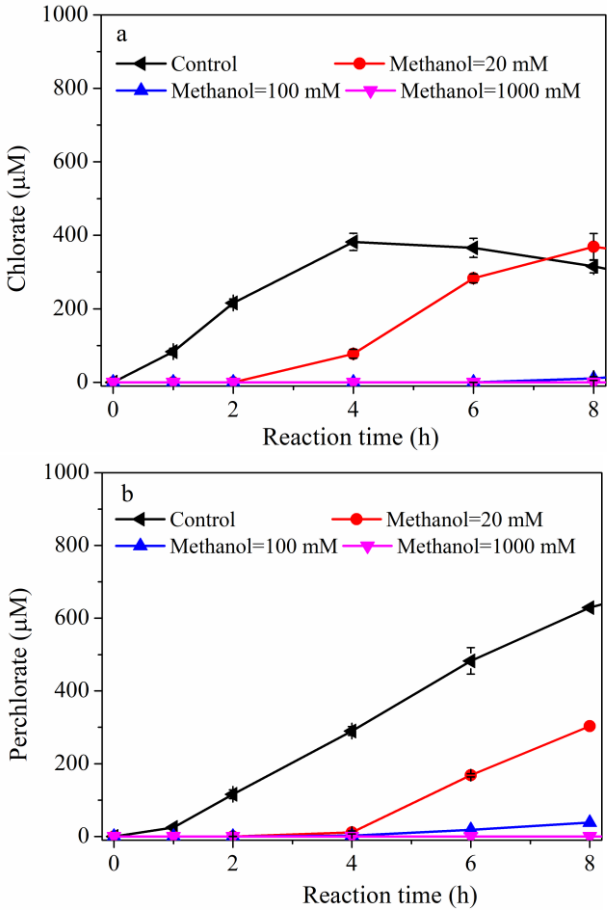

Fig. 4 Effect of methanol on the formation of ClO_3^- (a) and ClO_4^- (b) during the oxidation of Cl^-. $[Cl^-]_0$= 1 mM, $[Na_2SO_4]$ = 100 mM, $[Methanol]_0$= 20-1000 mM, current density = 10 $mA\cdot cm^{-2}$. Error bars mean standard deviation of replicates.

$$Cl^{\bullet} + HO^{\bullet} \xrightarrow{-H^{+}} OCl^{-} \quad \text{(R1)}$$

$$OCl^{-} \xrightarrow{-e,+HO^{\bullet},-H^{+}} ClO_2^{-} \xrightarrow{-e,+HO^{\bullet},-H^{+}} ClO_3^{-} \xrightarrow{-e,+HO^{\bullet},-H^{+}} ClO_4^{-} \quad \text{(R2)}$$

$$HO^{\bullet} + Cl^{-} \leftrightarrow ClHO^{\bullet -} \qquad k = 4.3 \times 10^{9}\ M^{-1}\cdot s^{-1} \quad \text{(R3)}$$

$$ClHO^{\bullet -} + H^{+} \rightarrow Cl^{\bullet} + H_2O \qquad k = 2.1 \times 10^{10}\ M^{-1}\cdot s^{-1} \quad \text{(R4)}$$

$$Cl^{\bullet} + Cl^{-} \leftrightarrow Cl_2^{\bullet -} \qquad k = 6.5 \times 10^{9}\ M^{-1}\cdot s^{-1} \quad \text{(R5)}$$

$$Cl^{\bullet} + Cl^{\bullet} \rightarrow Cl_2 \qquad k = 8.8 \times 10^{7}\ M^{-1}\cdot s^{-1} \quad \text{(R6)}$$

$$Cl_2 + H_2O \rightarrow Cl^{-} + HOCl + H^{+} \qquad k = 15\ M^{-1}\cdot s^{-1} \quad \text{(R7)}$$

3.4. Impact of different regeneration salts on PFASs recovery

A concern associated with using EO to treat chloride-containing still bottoms is the formation of ClO_3^- and ClO_4^-, which are generated when Cl^- is oxidized by $HO^{\bullet}$ on the Ti_4O_7 anode surface. One option to minimize the formation of ClO_3^- and ClO_4^- is to use a Cl^- free salt for IXR regeneration. Therefore, five salts were evaluated in this study in addition to NaCl to regenerate one same batch of PFAS-loaded IXR, including NaOH, $NaHCO_3$, Na_2SO_4, Na_2CO_3, and NaI. All regenerant solutions consisted of an 80% by volume methanol concentration with 2% by weight salt, except for Na_2CO_3 because of its low solubility in 80% methanol; therefore, a Na_2CO_3 concentration of 0.2% by weight was used. The mass distributions of major PFASs in the spent regenerants containing different salts are compared in Fig. 5. As shown, the total PFASs concentration was the highest when NaCl and NaI were used as the regenerant salts. For example, the elution of PFOS by NaCl and NaI reached 4.8 mg/L and 6.8 mg/L, respectively. However, only 0.5-1.7 mg/L PFOS was eluted when the other salts were used in the regeneration process at the same condition. Therefore, NaI may serve as a Cl^- free regenerant salt without compromised capability in PFASs recovery.

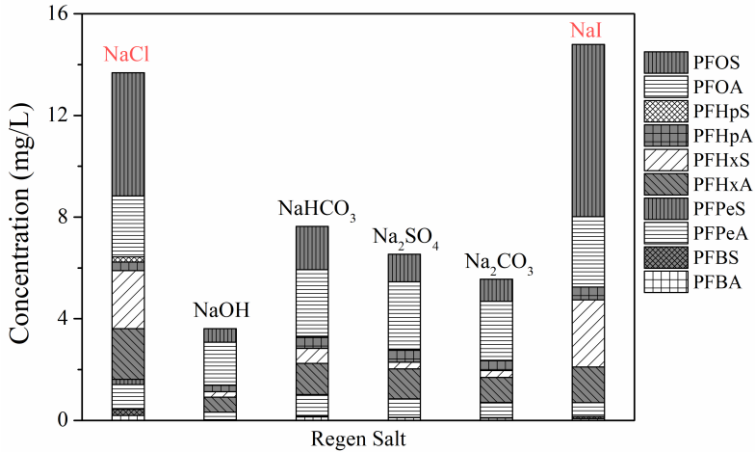

Fig. 5 PFASs eluted during IXR regeneration by regenerants containing different salts

3.5. PFASs degradation in still bottoms II

The spent regenerant containing NaI was further distilled to produce still bottoms II. EO treatment of still bottoms II was then performed with Ti_4O_7 anode to evaluate PFASs degradation and formation of ClO_3^- and ClO_4^- in this system. As listed in Table 1 and Table A1, still bottoms II contained high concentrations of PFOS (12.03 mg/L), PFOA (11.92 mg/L), and TOC (201,529 mg/L). It also contained quite a high concertation of chloride (3,579.1 mg/L), likely resulting from the concentration of the chloride contained in the groundwater through the IXR process but was significantly reduced from that in still bottoms I (62,716.0 mg/L).

As shown in Fig. 6, Ti_4O_7-based EO led to effective PFAAs degradation in still bottoms II. Therefore, the use of NaI as a regenerant did not negatively impact PFAAs degradation. After 200 h of treatment, the removal of PFOA, PFOS, PFBA, PFBS, PFPeA, PFPeS, PFHxA, PFPeS, PFHpA, PFHxS reached 98.7%, 96.5%, 86.8%, 99.7%, 99.90%, 99.9%, 97.1%, 99.9%, 99.9%, 98.9%, respectively (Table A1). The total removal of all these 10 monitored PFAAs was 60.9% at 50 h and reached 98.1% at 200 h of treatment. The time course data of all 10 monitored PFAAs are shown in Fig. S6, and their pseudo-first order degradation rate constant k_{SA} values are listed in Table A2. No appreciable ClO_3^- and ClO_4^- was detected in samples collected during EO treatment from 0 to100 h, while those in the sample collected at 200 h treatment were not analyzed.

It appeared that PFAAs degradation in still bottoms II was slower than those obtained in still bottoms I. This may be partially attributable to the higher organic matter content in still bottoms II than that in still bottoms I. As seen in Table A2, the surface area normalized rate constants (k_{SA}) obtained for PFASs in still bottoms II were lower than those obtained for the laboratory prepared solution of mixture PFASs by one to two orders of magnitude, also attributable to the interference of the high organic matter content present in still bottoms. It should be noted that the IXR process transfers PFASs from contaminated water to still bottoms with a huge volume reduction. In our test, the volume reduction was estimated to be 20,333 fold according to the IXR operation procedure described in section 2.2. Therefore, the advantage of applying EO to the concentrated still bottoms is evident in spite of the compromised PFASs degradation rate constants. Similar to Still Bottoms I, the original dark brown color of still bottoms II became clear and nearly colorless after 200 h of EO treatment (Fig. A3 b). The pH value was reduced from 9.64 to 8.33 in still bottoms II.

Additional target PFASs have been monitored for the experiment with still bottom II (See Table A3), and 6:2 FtS as a PFAAs precursor has been detected. Its degradation during the EO was also evident, reaching 96.1% after 200 h of treatment, and the time course data of 6:2 FtS are also included in Fig. A6. The F^-concentration after 50 h of EO treatment in this test was 5.25 mg/L. The defluorination ratio (F_r), the ratio between the released fluoride ion to the total fluorine in degraded PFASs, was 16.0% at 50 h of EO treatment. F^- became undetectable after 200 h of treatment. This may in part due to matrix effect that have interfered with fluoride analysis. We have later improved the protocol used for fluoride analysis and obtained a better recovery, which will be discussed in 3.7.

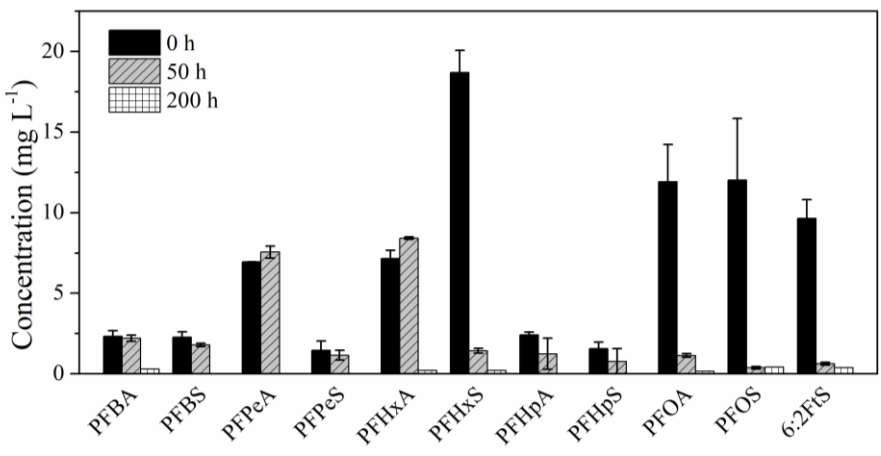

Fig. 6 Degradation of 10 PFAAs and precursor in still bottom II by electrooxidation treatment on Ti_4O_7 electrode. Current density = 10 mA·cm^{-2}. Error bars mean standard deviation of replicates.

3.6 Persulfate treatment

Persulfate treatment of still bottoms I sample was tested with different concentrations of persulfate activated at 60^{o} C, and the result is shown in Fig A8. Effective reduction of the total organic carbon (TOC) was achieved by persulfate treatment and it is dependent on the persulfate dosage. TOC dropped from 13,591 ppm to 8,473 ppm after 24 hours of treatment with 200-mM persulfate, marking a 38% reduction. Further, an additional experiment was performed to test the effect of persulfate pretreatment on the efficiency of EO treatment in which still bottoms I sample was first treated by 200-mM persulfate for 24 hours and then the treated solution was subject to EO treatment at 10 mA cm^{-2} for 168 hrs. The treatment efficiency is shown in Fig 7, and the result is compared to that obtained from the EO treatment of still bottoms II (without persulfate pretreatment) for 200 hrs, as the result of only EO treatment of still bottoms I sample for a similar time interval was not available. It appears that persulfate pretreatment did not help with PFAS removal. This is probably because EO treatment by itself can effectively degrade TOC, so that the effect of TOC removal by persulfate pretreatment on PFAS degradation during EO is limited. Formation of chlorate and perchlorate was observed during EO treatment of the still bottom I sample that had been subjected to persulfate treatment (Fig A9), which appears to be more than what was formed during EO treatment of the still bottom I sample without persulfate pretreatment (Fig 3). This is probably because persulfate treatment may selectively remove organic matter that have strong reactivity towards active chlorine, such as alcohols, and thus enhanced the formation of chlorate and perchlorate formation during EO treatment. Therefore, it is not recommended to use a persulfate pretreatment prior to the EO treatment of still bottoms.

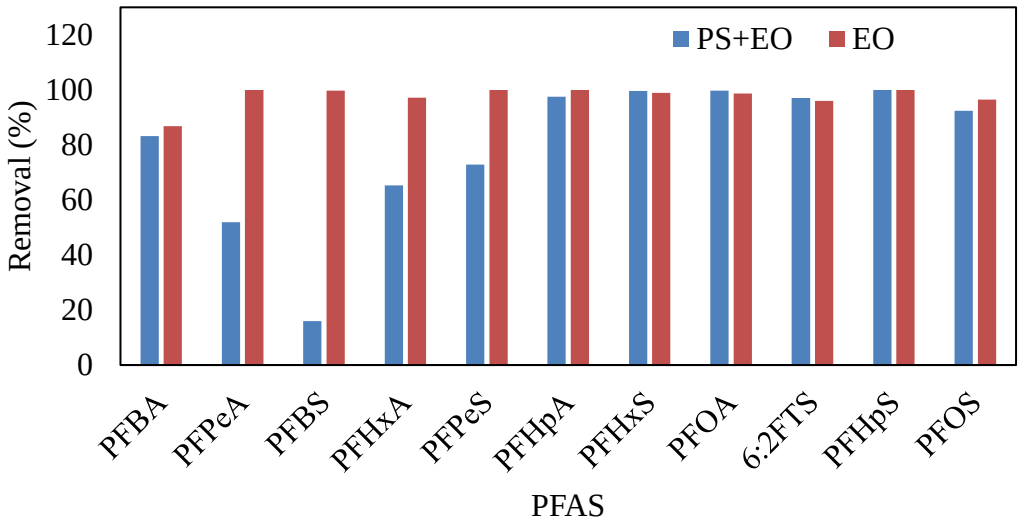

Fig. 7 PFAS removal in still bottoms I by persulfate treatment at 200-mM for 24 hours followed by EO treatment for 168 hours (PS+EO) in comparison to that in still bottoms II by only EO treatment (EO) for 200 hours

3.7 Additional test

The research team is currently performing a pilot scale test of the proposed IXR-EO treatment train on a contaminated as part of a project supported by AFCEC (BAA 108). One still bottom sample has been sent to Dr. Huang's laboratory for testing. This sample was generated using the MeOH/NaI regenerant following the general protocol described in 2.2. This sample is called still bottoms III in this report and its property is shown in Table A6. This sample is subjected to EO treatment as described in 2.3, and the results are shown in Fig 8 and Table A7. Great PFAS removal was achieved, consistent with the result obtained with still bottoms II (shown in Fig 6). The TOC of still bottoms III decreased steadily over time during the EO treatment (Fig A10). An improved method was used in this experiment to quantify fluoride in the solution. The sample at the end of EO treatment was diluted 100 times and then analyzed for F^- using a standard addition approach to minimize the interference of matrix effect (see Text A3 for detail). The fluoride concentration was found to be 30.55 ± 0.03 (ppm), and this accounted for a 32.33% defluorination ratio (F_r). Although the fluoride analysis was improved and a higher defluorination ratio was obtained than those measured for still bottoms I and II described above, it was still relatively low compared to the result obtained for a solution prepared by spiking PFAAs in pure water in our previous study [46], in which the defluorination ratios after 8 h treatment were consistently above 90% when the current density was above 10 $mA \cdot cm^{-2}$. The low fluoride concentration detected may still be caused by the analytical difficulty associated with the complex still bottoms matrix, even when the method has been improved. Alternatively, it may also result from fluoride binding with certain constituents in the solution, such as metal cations, or simply low defluorination over the EO process, which requires further investigation.

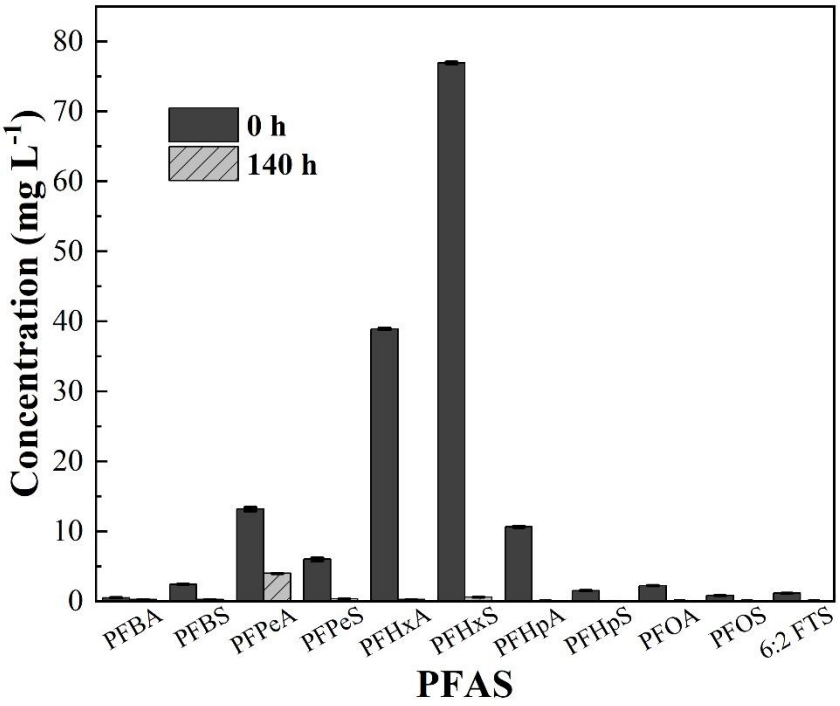

Fig. 8 Degradation of PFAAs in still bottom III during electrochemical oxidation treatment on Ti_4O_7 electrode. Current density = 10 mA·cm^{-2}. Error bars mean standard deviation of replicates. The values are also listed in Table A8.

4. Conclusion

The results of this study highlight the potential of electrooxidation for the effective treatment of PFASs in still bottoms using a Magnéli phase Ti_4O_7 anode. In still bottoms I (MeOH/NaCl regenerant for IXR regeneration), the total removal of the 10 monitored PFAAs compounds was 60.9% after 40 h of EO treatment, with the degradation of PFOA and PFOS over 90.0% (Table A1). Oxidation of Cl^- led to the formation of ClO_3^- and ClO_4^- in this solution. The study demonstrates residual methanol in the still bottom can inhibit the formation of ClO_3^- and ClO_4^-, because methanol can quench chlorine radicals, but did not impede the degradation of PFAAs by EO. The total removal of all 10 monitored PFAAs was 98.1% at 200 h of treatment in still bottoms II, which used NaI instead of NaCl as the regenerant salt (Table A1). No formation of ClO_3^- and ClO_4^- was observed in this system, although chloride was detected in still bottom II. Our study indicates the combination of regenerable IXR technology and EO using a Magnéli phase Ti_4O_7 anode shows appreciable promise for removing PFASs from water and destroying the PFASs onsite, thereby minimizing the expense and liability associated with disposing of the PFASs containing waste. Persulfate pretreatment did not appear to enhance the degradation of PFAS during EO treatment. However, persulfate pretreatment could selectively remove organic matter capable of quenching chlorine radical, and thus help with the formation of

chlorate and perchlorate. Therefore, it is not recommended to use a persulfate pretreatment prior to the EO treatment of still bottoms.

5 Publications and future plans

5.1 publications

Five papers have been published as a result of the support in part by this project, which are listed below.

- Wang L., Nickelsen M., Chiang S., Woodard S., Wang Y., Liang, S., Huang, Q., 2020, Treatment of Perfluoroalkyl Acids in Concentrated Wastes from Regeneration of Spent Ion Exchange Resin by Electrochemical Oxidation using Magnéli Phase Ti4O7 Anode. *Chemical Engineering Journal Advances*, 100078.
- Wang Y., Shi H., Li C., & Huang Q., 2020, Electrochemical degradation of perfluoroalkyl acids by titanium suboxide anodes. *Environmental Science: Water Research & Technology*, *6*(1), 144-152.
- Wang L., Lu J., Li L., Wang Y., & Huang, Q., 2020, Effects of chloride on electrochemical degradation of perfluorooctanesulfonate by Magnéli phase Ti_4O_7 and boron doped diamond anodes. *Water Research, 170*, 115254.
- Yang P., Wang Y., Lu J., Tishchenko V., Huang Q., 2020, Electrochemical Oxidation of Perfluorooctanesulfonate by Magnéli Phase Ti_4O_7 Electrode in the Presence of Trichloroethylene, *Advanced Environmental Engineering Research*, *1*(4), 2004006.
- Shi H., Wang Y., Li C., Pierce R., Gao S., & Huang Q., 2019, Degradation of Perfluorooctanesulfonate by Reactive Electrochemical Membrane Composed of Magneli Phase Titanium Suboxide. *Environmental Science & Technology*, *53*(24), 14528-14537.

5.2 Future research plans

The results of this project indicate the potential of Magneli phase titanium suboxide (TSO) ceramic materials for applications in EO treatment to degrade PFAS in still bottoms. The results provide a basis for coupling IXR and Ti_4O_7-based EO technologies as an integral solution of PFASs contaminated waters. This project study was performed with bench scale batch reactors. The promise shown in this study warrants pilot scale demonstrations of the system, as well as further scaling up and system integration efforts. One such demonstration is currently under way in support by AFCEC (BAA 108), and the result will be reported when the test is complete. In addition, there is potential to further enhance the intrinsic reactivity of the titanium suboxide anode towards PFAS and to reduce its reactivity towards chloride by modifying the materials and improving reactor design (e.g., using reactive electrochemical membrane reactor). The PI is currently working on this under SERDP support (ER-2717), and the improved EO systems are expected to have greater performance for degrading PFAS in still bottoms.

6. References

[1] H. Lin, J. Niu, S. Liang, C. Wang, Y. Wang, F. Jin, Q. Luo, Q. Huang, Development of macroporous Magnéli phase Ti_4O_7 ceramic materials: As an efficient anode for mineralization of poly- and perfluoroalkyl substances, Chemical Engineering Journal 354 (2018) 1058-1067.

[2] M. Kotthoff, J. Muller, H. Jurling, M. Schlummer, D. Fiedler, Perfluoroalkyl and polyfluoroalkyl substances in consumer products, Environmental Science and Pollution Research 22 (2015) 14546-14559.

[3] F. Ye, Y. Zushi, S. Masunaga, Survey of perfluoroalkyl acids (PFAAs) and their precursors present in Japanese consumer products, Chemosphere 127 (2015) 262-268.

[4] H. Lin, Y. Wang, J. Niu, Z. Yue, Q. Huang, Efficient sorption and removal of perfluoroalkyl acids (PFAAs) from aqueous solution by metal hydroxides generated in situ by electrocoagulation, Environmental Science and Technology 49 (2015) 10562-10569.

[5] E. Kissa, Fluorinated Surfactants and Repellents, Marcel Dekker, New York. (2011).

[6] L. Jin, P. Zhang, T. Shao, S. Zhao, Ferric ion mediated photodecomposition of aqueous perfluorooctane sulfonate (PFOS) under UV irradiation and its mechanism, Journal of Hazardous Materials 271 (2014) 9-15.

[7] J. Niu, H. Lin, J. Xu, H. Wu, Y. Li, Electrochemical mineralization of perfluorocarboxylic acids (PFCAs) by ce-doped modified porous nanocrystalline PbO_2 film electrode, Environmental Science and Technology 46 (2012) 10191-10198.

[8] J.M. Conder, R.A. Hoke, W.d. Wolf, M.H. Russell, R.C. Buck, Are PFCAs bioaccumulative? A critical review and comparison with regulatory criteria and persistent lipophilic compounds, Environmental Science and Technology 42 (2008) 995-1003.

[9] D. Zhang, Q. Luo, B. Gao, S.Y. Chiang, D. Woodward, Q. Huang, Sorption of perfluorooctanoic acid, perfluorooctane sulfonate and perfluoroheptanoic acid on granular activated carbon, Chemosphere 144 (2016) 2336-2342.

[10] P. Zareitalabad, J. Siemens, M. Hamer, W. Amelung, Perfluorooctanoic acid (PFOA) and perfluorooctanesulfonic acid (PFOS) in surface waters, sediments, soils and wastewater - a review on concentrations and distribution coefficients, Chemosphere 91 (2013) 725-732.

[11] C. Gallen, D. Drage, G. Eaglesham, S. Grant, M. Bowman, J.F. Mueller, Australia-wide assessment of perfluoroalkyl substances (PFASs) in landfill leachates, Journal of Hazardous Materials 331 (2017) 132-141.

[12] A.B. Lindstrom, M.J. Strynar, E.L. Libelo, Polyfluorinated compounds: past, present, and future, Environmental Science and Technology 45 (2011) 7954-7961.

[13] Q. Zhuo, S. Deng, B. Yang, J. Huang, B. Wang, T. Zhang, G. Yu, Degradation of perfluorinated compounds on a boron-doped diamond electrode, Electrochimica Acta 77 (2012) 17-22.

[14] J.F. Niu, Y. Li, E.X. Shang, Z.S. Xu, J.Z. Liu, Electrochemical oxidation of perfluoried compounds in water, Chemosphere 146 (2016) 526-538.

[15] M.F. Rahman, S. Peldszus, W.B. Anderson, Behaviour and fate of perfluoroalkyl and polyfluoroalkyl substances (PFASs) in drinking water treatment: a review, Water Research 50 (2014) 318-340.

[16] N. Merino, Y. Qu, R.A. Deeb, E.L. Hawley, M.R. Hoffmann, S. Mahendra, Degradation and Removal Methods for Perfluoroalkyl and Polyfluoroalkyl Substances in Water, Environmental Engineering Science 33 (2016) 615-649.

[17] K.E. Carter, J. Farrell, Removal of Perfluorooctane and Perfluorobutane Sulfonate from Water via Carbon Adsorption and Ion Exchange, Separation Science and Technology 45 (2010) 762-767.

[18] A. Soriano, D. Gorri, A. Urtiaga, Efficient treatment of perfluorohexanoic acid by nanofiltration followed by electrochemical degradation of the NF concentrate, Water Research 112 (2017) 147-156.

[19] A. Soriano, D. Gorri, L.T. Biegler, A. Urtiaga, An optimization model for the treatment of perfluorocarboxylic acids considering membrane preconcentration and BDD electrooxidation, Water Research 164 (2019) 114954.

[20] Á. Soriano, D. Gorri, A. Urtiaga, Selection of High Flux Membrane for the Effective Removal of Short-Chain Perfluorocarboxylic Acids, Industrial & Engineering Chemistry Research 58 (2019) 3329-3338.

[21] I. Ross, J. McDonough, J. Miles, P. Storch, P. Thelakkat Kochunarayanan, E. Kalve, J. Hurst, S. S. Dasgupta, J. Burdick, A review of emerging technologies for remediation of PFASs, Remediation Journal 28 (2018) 101-126.

[22] S. Woodard, J. Berry, B. Newman, Ion exchange resin for PFAS removal and pilot test comparison to GAC, Remediation Journal 27 (2017) 19-27.

[23] C.E. Schaefer, C. Andaya, A. Burant, C.W. Condee, A. Urtiaga, T.J. Strathmann, C.P. Higgins, Electrochemical treatment of perfluorooctanoic acid and perfluorooctane sulfonate: insights into mechanisms and application to groundwater treatment, Chemical Engineering Journal 317 (2017) 424-432.

[24] K.E. Carter, J. Farrell, Oxidative destruction of perfluorooctane sulfonate using boron-doped diamond film electrodes, Environmental Science and Technology 42 (2008) 6111- 6115.

[25] H. Lin, J. Niu, J. Xu, H. Huang, D. Li, Z. Yue, C. Feng, Highly efficient and mild electrochemical mineralization of long-chain perfluorocarboxylic acids (C_9-C_{10}) by Ti/SnO_2-Sb-Ce, Ti/SnO_2-Sb/Ce-PbO_2, and Ti/BDD electrodes, Environmental Science and Technology 47 (2013) 13039-13046.

[26] H. Lin, J. Niu, S. Ding, L. Zhang, Electrochemical degradation of perfluorooctanoic acid (PFOA) by Ti/SnO_2-Sb, Ti/SnO_2-Sb/PbO_2 and Ti/SnO_2-Sb/MnO_2 anodes, Water Research 46 (2012) 2281-2289.

[27] A.M. Trautmann, H. Schell, K.R. Schmidt, K.M. Mangold, A. Tiehm, Electrochemical degradation of perfluoroalkyl and polyfluoroalkyl substances (PFASs) in groundwater, Water Science and Technology 71 (2015) 1569-15675.

[28] A. Soriano, C. Schaefer, A. Urtiaga, Enhanced treatment of perfluoroalkyl acids in groundwater by membrane separation and electrochemical oxidation, Chemical Engineering Journal Advances 4 (2020).

[29] J. Radjenovic, D.L. Sedlak, Challenges and opportunities for electrochemical processes as next-generation technologies for the treatment of contaminated water, Environmental Science and Technology 49 (2015) 11292-112302.

[30] A.Y. Bagastyo, D.J. Batstone, K. Rabaey, J. Radjenovic, Electrochemical oxidation of electrodialysed reverse osmosis concentrate on Ti/Pt-IrO_2, Ti/SnO_2-Sb and boron-doped diamond electrodes, Water Research 47 (2013) 242-250.

[31] C.E. Schaefer, C. Andaya, A. Urtiaga, E.R. McKenzie, C.P. Higgins, Electrochemical treatment of perfluorooctanoic acid (PFOA) and perfluorooctane sulfonic acid (PFOS) in groundwater impacted by aqueous film forming foams (AFFFs), Journal of Hazardous Materials 295 (2015) 170-175.

[32] F.C. Walsh, R.G.A. Wills, The continuing development of Magnéli phase titanium sub-oxides and Ebonex® electrodes, Electrochimica Acta 55 (2010) 6342–6351.

[33] S.O. Ganiyu, N. Oturan, S. Raffy, M. Cretin, R. Esmilaire, E. van Hullebusch, G. Esposito, M.A. Oturan, Sub-stoichiometric titanium oxide (Ti_4O_7) as a suitable ceramic anode for electrooxidation of organic pollutants: a case study of kinetics, mineralization and toxicity assessment of amoxicillin, Water Research 106 (2016) 171-182.

[34] P. Geng, J. Su, C. Miles, C. Comninellis, G. Chen, Highly-ordered magnéli Ti_4O_7 nanotube arrays as effective anodic material for electro-oxidation, Electrochimica Acta 153 (2015) 316-324.

[35] O.I. Kasian, T.V. Luk'yanenko, P. Demchenko, R.E. Gladyshevskii, R. Amadelli, A.B. Velichenko, Electrochemical properties of thermally treated platinized Ebonex® with low content of Pt, Electrochimica Acta 109 (2013) 630-637.

[36] G. Kreysa, K.-i. Ota, R.F. Savinell, Pollutants in water-electrochemical remediation using ebonex electrodes, Encyclopedia of applied electrochemistry (2014) 1629-1633.

[37] M. Toyoda, T. Yano, B. Tryba, S. Mozia, T. Tsumura, M. Inagaki, Preparation of carbon-coated Magneli phases Ti_nO_{2n-1} and their photocatalytic activity under visible light, Applied Catalysis B: Environmental 88 (2009) 160-164.

[38] C. Yao, F. Li, X. Li, D. Xia, Fiber-like nanostructured Ti_4O_7 used as durable fuel cell catalyst support in oxygen reduction catalysis, Journal of Materials Chemistry 22 (2012) 16560-16565.

[39] A.M. Zaky, B.P. Chaplin, Porous substoichiometric TiO_2 anodes as reactive electrochemical membranes for water treatment, Environmental Science and Technology 47 (2013) 6554-6563.

[40] A.M. Zaky, B.P. Chaplin, Mechanism of *p*-substituted phenol oxidation at a Ti_4O_7 reactive electrochemical membrane, Environmental Science and Technology 48 (2014) 5857-5867.

[41] G. Chen, E.A. Betterton, R.G. Arnold, Electrolytic oxidation of trichloroethylene using a ceramic anode, Journal of Applied Electrochemistry 29 (1999) 961-970.

[42] G. Chen, E.A. Betterton, R.G. Arnold, Electrolytic reduction of trichloroethylene and chloroform at a Pt- or Pd-coated ceramic cathode, Journal of Applied Electrochemistry 33 (2003) 161–169.

[43] S. Liang, H. Lin, X. Yan, Q. Huang, Electro-oxidation of tetracycline by a magnéli phase Ti_4O_7 porous anode: kinetics, products, and toxicity, Chemical Engineering Journal 332 (2018) 628-636.

[44] S. Liang, R.D. Pierce, H. Lin, S.-Y.D. Chiang, Q.J. Huang, Electrochemical oxidation of PFOA and PFOS in concentrated waste streams, Remediation Journal 28 (2018) 127-134.

[45] L. Wang, J. Lu, L. Li, Y. Wang, Q. Huang, Effects of chloride on electrochemical degradation of perfluorooctanesulfonate by Magneli phase Ti_4O_7 and boron doped diamond anodes, Water Research 170 (2020) 115254.

[46] Y. Wang, R.D. Pierce, H. Shi, C. Li, Q. Huang, Electrochemical degradation of perfluoroalkyl acids by titanium suboxide anodes, Environmental Science: Water Research & Technology 6 (2020) 144-152.

[47] H. Shi, Y. Wang, C. Li, R. Pierce, S. Gao, Q. Huang, Degradation of perfluorooctanesulfonate by reactive electrochemical membrane composed of magneli phase titanium suboxide, Environmental Science and Technology 53 (2019) 14528-14537.

[48] Y.J. Jung, K.W. Baek, B.S. Oh, J.W. Kang, An investigation of the formation of chlorate and perchlorate during electrolysis using Pt/Ti electrodes: the effects of pH and reactive oxygen species and the results of kinetic studies, Water Research 44 (2010) 5345-5355.

[49] R. Srinivasan, G.A. Sorial, Treatment of perchlorate in drinking water: a critical review, Separation and Purification Technology 69 (2009) 7-21.

[50] Orchideh Azizi, David Hubler, Glenn Schrader, James Farrell, B.P. Chaplin, Mechanism of perchlorate formation on boron-doped diamond film anodes, Environmental Science and Technology 45 (2011) 10582–10590.

[51] E.T. Urbansky, Perchlorate as an environmental contaminant, Environmental Science and Pollution Research 9 (2002) 187-192.

[52] M.E.H. Bergmann, A.S. Koparal, T. Iourtchouk, Electrochemical advanced oxidation processes, formation of halogenate and perhalogenate species: a critical review, Critical Reviews in Environmental Science and Technology 44 (2014) 348-390.

[53] Nickelsen M. G. , W.S. E., Sustainable system and method for removing and concentrating per- and polyfluoroalkyl substances (PFAS) from water, (2017).

[54] B. Gomez-Ruiz, S. Gómez-Lavín, N. Diban, V. Boiteux, A. Colin, X. Dauchy, A. Urtiaga, Efficient electrochemical degradation of poly- and perfluoroalkyl substances (PFASs) from the

effluents of an industrial wastewater treatment plant, Chemical Engineering Journal 322 (2017) 196-204.

[55] C.E. Schaefer, D. Tran, Y. Fang, Y.J. Choi, C.P. Higgins, T.J. Strathmann, Electrochemical treatment of poly- and perfluoroalkyl substances in brines, Environmental Science: Water Research & Technology (2020).

[56] G. Perez, J. Saiz, R. Ibanez, A.M. Urtiaga, I. Ortiz, Assessment of the formation of inorganic oxidation by-products during the electrocatalytic treatment of ammonium from landfill leachates, Water Research 46 (2012) 2579-2590.

[57] A. Donaghue, B.P. Chaplin, Effect of select organic compounds on perchlorate formation at boron-doped diamond film anodes, Environmental Science and Technology 47 (2013) 12391-12399.

[58] S. Hou, L. Ling, D.D. Dionysiou, Y. Wang, J. Huang, K. Guo, X. Li, J. Fang, Chlorate formation mechanism in the presence of sulfate radical, chloride, bromide and natural organic matter, Environmental Science and Technology 52 (2018) 6317-6325.

[59] S. Gligorovski, R. Strekowski, S. Barbati, D. Vione, Environmental implications of hydroxyl radicals (•OH), Chemical Reviews 115 (2015) 13051-13092.

7. Appendix

Text A1

Electrode fabrication and characterization

The Magnéli phase Ti_4O_7 electrode was fabricated through a high temperature sintering process as described in our previous study [1]. In brief, TiO_2 powder was heated at 950 ˚C and reduced to Ti_4O_7 powder under controlled H_2 flow. The Ti_4O_7 powder was mixed (0.5%, m/m) with polyacrylamide/polyvinyl alcohol (95/5, m/m) to form a slurry that was then spray-dried to form ceramic granulates. The ceramic granulates were then pressed to make a ceramic preform that was dried and then sintered at 1350 °C in a vacuum for 11 h to form a bulk electrode.

The chemical composition of the Magnéli phase Ti_4O_7 electrode was characterized using an X'Pert PRO MRD X-ray diffractometer (XRD) (PANalytical, Netherlands) with CuKα1 radiation at 40 kV/40 mA. The surface morphology of Ti_4O_7 electrode was examined using scanning electron microscopy (SEM) on a Hitachi's-4800 FE-SEM system (Hitachi, Japan). The porosimetry analysis of the anode was measured using a Micromeritics Autopore IV 9500 mercury porosimeter (Norcross, GA) according to method ISO 15901-1.

The XRD pattern confirmed Magnéli phase Ti_4O_7 as the dominant composition of the electrode material (Fig. A7 A and B). The SEM image (Fig. A7 C) shows fairly uniform interconnecting pores with diameters smaller than 10 µm on the surface of Magnéli phase Ti_4O_7 anode material. Mercury intrusion porosimetry analysis (Fig. A7 D) indicates a porosity of 21.6%, and a median pore diameter of 3.6 µm (based on volume) or 2.8 µm (based on area), and an average pore diameter of 2.6 µm.

Text A2

UPLC-MS/MS method

The target PFASs and the isotope-labeled internal standards are listed in Table S3 Electrospray ionization (ESI) was operated in a negative mode with capillary voltage at 1.14 kV, cone voltage 60 V, source temperature at 400 °C and desolation temperature at 550 °C. The mass transitions and spectrometry conditions for Multiple Reaction Monitoring (MRM) monitoring are specified in Table S4. Quantification of a target PFASs was achieved by internal standard calibration. The UPLC was operated with UPLC grade methanol (A) obtained from Sigma Aldrich and water (B) (5 mM ammonium acetate) as the mobile phases at a flow rate of 0.3 mL/min using a gradient condition listed in Table S5. The major QA/QC measures include: A signal-to-noise (S/N) Ratio must be ≥ 10:1; the %RSD of the RFs for all analytes must be < 20%. Linear calibrations must have an $r^2 \geq 0.99$ for each analyte; and analytes must be within ±30% of their true value for each calibration standard.

Text A3

Fluoride detection by standard addition

All still bottom samples were diluted 100 times by DI water prior to IC analysis. F^- in the diluted sample was then analyzed using a standard addition approach as described in Principles of Instrumental Analysis (Skoog, D. A.; Holler, F. J.; Nieman, T. A.. 5th ed. 1998). In short, 5 mL of a diluted sample was placed in a series of 10 mL volumetric tubes. Exactly 0, 0.05, 0.10, 0.15 or 0.25 mL of a standard solution containing 100 ppm of F^- (C_s) was added to each. After dilution to volume, each of the five solutions was analzyed using IC by the method described in 2.4 and the response is denoted as (S). The IC response S and the volume of the added standard solution V_s were fitted to the linear equation $S = mV_s + b$, to obtain the slope m. Then the concentration of the sample c_x can be calculated by $c_x = \frac{b \cdot c_s}{m \cdot V_x}$, where V_x is the volume of the sample solution (5.0 mL).

Table A1. Concentrations of PFASs in still bottom samples before and after EO treatment (mg/L).

	PFAAs	Still bottom I			Still bottom II		
		Initial concentration	Final concentration	Removal percentage	Initial concentration	Final concentration	Removal percentage
1	PFBA	1.66	2.48	-49.6	2.32	0.31	86.8
2	PFBS	1.45	1.55	-6.8	2.29	0.01	99.7
3	PFPeA	10.10	11.13	-10.2	6.95	<LOQ*	100
4	PFPeS	2.64	2.36	10.8	1.46	<LOQ	100
5	PFHxA	13.16	14.07	-6.9	7.17	0.21	100
6	PFHxS	40.94	2.03	95.0	18.71	0.21	100
7	PFHpA	3.69	1.60	56.6	2.42	<LOQ	100
8	PFHpS	2.58	0.08	96.8	1.57	<LOQ	100
9	PFOA	7.56	0.39	94.8	11.92	0.15	98.7
10	PFOS	8.08	0.09	98.9	12.02	0.42	96.5
11	6:2 FTS*	-	-	-	9.64	0.38	96.1

*Only included in analysis of still bottom II.

*LOQ: limit of quantification.

Table A2 k_{SA} (m s^{-1}) for each PFASs tested in experiments

	PFCs	Still bottom I	Still bottom II	Mixture in 100 mM Na_2SO_4*
1	PFOS	1.71×10^{-7}	1.66×10^{-7}	1.11×10^{-5}
2	PFOA	1.71×10^{-7}	8.19×10^{-8}	4.09×10^{-6}
3	PFHxS	1.26×10^{-7}	5.06×10^{-8}	2.58×10^{-6}
4	PFHpA	3.38×10^{-8}	1.21×10^{-8}	1.62×10^{-6}
5	PFHpS	1.30×10^{-7}	3.67×10^{-8}	-
6	PFBS		5.38×10^{-8}	1.59×10^{-7}
7	PFBA		2.60×10^{-8}	7.49×10^{-8}
8	PFPeA		2.74×10^{-8}	1.19×10^{-7}
9	PFPeS		1.21×10^{-8}	-
10	PFHxA		2.74×10^{-8}	3.42×10^{-7}
11	6:2 FtS		1.44×10^{-7}	

Table A3. The target PFASs and the isotope-labeled internal standards

	PFAA standards	Isotope-labeled internal standards
1	perfluoro-n-butanoic acid (PFBA)	perfluoro-n-[$^{13}C_4$]butanoic acid (MPFBA)
2	perfluoro-n-pentanoic acid (PFPeA)	perfluoron-[$^{13}C_5$]pentanoic acid (M5PFPeA)
3	perfluoro-nhexanoic acid (PFHxA)	perfluoro-n-[1,2,3,4,6-$^{13}C_5$]hexanoic acid (M5PFHxA)
4	perfluoro-n-heptanoic acid (PFHpA)	perfluoro-n-[1,2,3,4-$^{13}C_4$]heptanoic acid (M4PFHpA)
5	perfluoro-n-octanoic acid (PFOA)	perfluoro-n- [$^{13}C_8$]octanoic acid (M8PFOA)
6	perfluoro-n-nonanoic acid (PFNA)	perfluoro-n-[$^{13}C_9$]nonanoic acid (M9PFNA)
7	perfluoro-n-decanoic acid (PFDA)	perfluoro-n-[1,2,3,4,5,6-$^{13}C_6$]decanoic acid (M6PFDA)
8	perfluoro-n-undecanoic acid (PFUdA)*	perfluoro-n- [1,2,3,4,5,6,7-$^{13}C_7$]undecanoic acid (M7PFUdA)
9	perfluoro-n-dodecanoic acid (PFDoA)*	perfluoro-n-[1,2-$^{13}C_2$]dodecanoic acid (MPFDoA)
10	perfluoro-n-tridecanoic acid (PFTrDA)*	perfluoro-n-[1,2-$^{13}C_2$]dodecanoic acid (MPFDoA)
11	perfluoro-n-tetradecanoic acid (PFTeDA)*	perfluoro-n-[1,2-$^{13}C_2$]tetradecanoic acid (M2PFTeDA)
12	perfluoro-1-butanesulfonate (PFBS)	nodium perfluoro-1- [2,3,4-$^{13}C_3$]butanesulfonate (M3PFBS)
13	perfluoro-1-pentanesulfonate (PFPeS)	sodium perfluoro-1-[1,2,3-$^{13}C_3$]hexanesulfonate (M3PFHxS)
14	perfluoro-1-hexanesulfonate (PFHxS)	sodium perfluoro-1-[1,2,3-$^{13}C_3$]hexanesulfonate (M3PFHxS)

15	perfluoro-1-heptanesulfonate (PFHpS)	perfluoro-[$^{13}C_8$]octanesulfonate (M8PFOS)
16	perfluoro-1-octanesulfonate (PFOS)	perfluoro-[$^{13}C_8$]octanesulfonate (M8PFOS)
17	perfluoro-1-nonanesulfonate (PFNS)	perfluoro-[$^{13}C_8$]octanesulfonate (M8PFOS)
18	perfluoro- 1-decanesulfonate (PFDS)	perfluoro-[$^{13}C_8$]octanesulfonate (M8PFOS)
19	perfluorooctanesulfonamide (FOSA)	perfluoro-1-[$^{13}C_8$]octanesulfonamide (M8FOSA)
20	fluorotelomer stearate monoester 8:2 (FTS 8:2)*	sodium 1H,1H,2H,2H-perfluoro-1-[1,2-$^{13}C^2$]decanesulfonate (M2-8:2FtS)
21	fluorotelomer sulfonate 6:2 (FtS 6:2)*	sodium 1H,1H,2H,2H-perfluoro-1-[1,2-$^{13}C^2$]octanesulfonate (M2-6:2FtS)
22	fluorotelomer sulfonic acid 4:2 (FtS 4:2)*	sodium 1H,1H,2H,2H-perfluoro-1-[1,2-$^{13}C_2$]hexanesulfonate (M2-4:2FtS)
23	2-(N-Ethylperfluorooctanesulfonamido) acetic acid (NEtFOSAA)*	N-ethyl-d5- perfluoro-1-octanesulfonamidoacetic acid (d5-N-EtFOSAA)
24	2-(N-Methylperfluorooctanesulfonamido) acetic acid (NMeFOSAA)*	N-methyl-d3- perfluoro-1octanesulfonamidoacetic acid (d3-N-MeFOSAA)

*Only included in analysis of still bottom II.

Table A4 Analyte-specific mass spectrometer parameters for PFASs

	PFCs	MRM	Dwell (s)	Cone (V)	Collision (eV)
1	PFBA	213.00>169.00	0.007	15.0	10.0
2	PFPeA	263.00>219.00	0.007	15.0	9.0
3	PFBS	299.00>80.00	0.007	56.0	26.0
4	PFHxA	313.00>269.00	0.007	15.0	8.0
5	4:2 FtS	327.00>307.00	0.009	25.0	20.0
6	PFPeS	349.00>80.00	0.009	45.0	25.0
7	PFHpA	363.00>319.00	0.007	15.0	7.0
8	PFHxS	399.00>80.10	0.009	45.0	40.0
9	PFOA	413.00>369.00	0.007	16.0	8.0
10	6:2 FtS	427.00>407.00	0.009	25.0	20.0
11	PFHpS	449.00>80.2.00	0.009	60.0	35.0
12	PFOS	498.78>80.20	0.009	60.0	35.0
13	PFDS	498.00>77.90	0.009	40.0	30.0
14	PFNA	463.00>418.90	0.009	20.0	10.0
15	PFDA	513.00>468.90	0.009	20.0	10.0
16	8:2 FtS	527.00>506.80	0.009	25.0	25.0
17	PFNS	549.00>80.20	0.009	65.0	45.0
18	PFUdA	563.00>518.90	0.009	18.0	10.0
19	NMeFOSAA	570.00>418.90	0.009	35.0	20.0
20	NEtFOSAA	584.00>418.80	0.009	35.0	20.0
21	PFDS	599.00>80.20	0.009	70.0	50.0
22	PFDoA	613.00>568.90	0.009	18.0	10.0
23	PFTrDA	663.00>618.90	0.009	22.0	15.0
24	PFTeDA	713.00>668.90	0.009	15.0	14.0

Table A5 The flow rate and the gradient condition of UPLC program.

Time (min)	Flow rate (mL min^{-1})	%A	%B	Curve
Initial	0.3	40.0	60.0	Initial
4	0.3	80.0	20.0	6
5	0.3	40.0	60.0	6

Table A6. Properties of still bottom III.

Property	Still Bottoms III
pH	10.18
Conductivity ($mS \cdot cm^{-1}$)	69.1
TOC (mg $C \cdot L^{-1}$)	16529.31
Methanol ($mg \cdot L^{-1}$)	5.64

Table A7. Degradation of PFAAs in still bottom III during electrochemical oxidation treatment on Ti_4O_7 electrode with time. Current density = 10 $mA \cdot cm^{-2}$. Error bars mean standard deviation of replicates.

PFAS	Concentration (mg L^{-1})			
	0 h	**40 h**	**80 h**	**140 h**
PFBA	487.96±15.04	491.13±17.28	3013.60±20.05	209.13±6.41
PFPeA	13128.21±283.04	5179.88±59.16	8583.24±51.69	3956.41±35.38
PFBS	2409.72±13.93	1800.00±5.66	1833.33±6.36	212.96±5.34
PFHxA	38887.10±116.23	29991.40±40.58	11274.19±12.05	216.59±2.85
PFPeS	5982.14±230.01	1809.75±49.67	2959.58±9.03	331.10±8.27
PFHpA	10624.47±96.16	2785.63±37.02	1682.69±7.90	44.45±3.76
PFHxS	76912.20±123.87	3708.82±55.44	2875.87±6.60	559.08±8.70
PFOA	2212.29±28.79	36.36±3.37	40.42±0.73	16.12±0.43
6:2 FTS	1131.90±29.77	90.03±3.65	69.12±0.97	34.63±0.78
PFHpS	1492.02±18.57	16.51±1.67	5.31±0.50	2.43±0.07
PFNA	53.32±2.28	7.54±0.13	5.14±0.07	3.72±0.40
FOSA	10.13±0.86	0.23±0.01	0.40±0.01	0.00±0.00
PFOS	812.40±9.80	12.72±0.32	27.64±0.57	12.40±0.98
PFDA	1.54±0.47	1.27±0.09	0.00±0.00	0.00±0.00
8:2 FTS	34.61±0.48	0.00±0.00	0.00±0.00	0.00±0.00
PFNS	4.86±0.08	0.79±0.05	0.36±0.01	0.00±0.00
PFUdA	9.54±0.88	2.22±0.05	0.00±0.00	0.00±0.00
PFDS	2.14±0.06	0.00±0.00	0.00±0.00	0.00±0.00

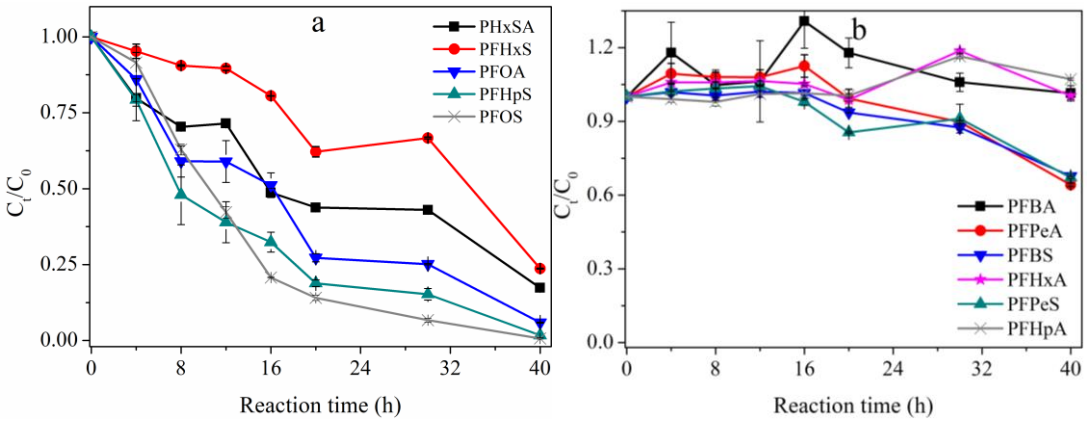

Fig. A1 Degradation of PFAAs in still bottom I during electrochemical oxidation treatment on Ti_4O_7 electrode with time. Current density = 10 mA·cm^{-2}, reaction time = 40 h. Error bars mean standard deviation of replicates.

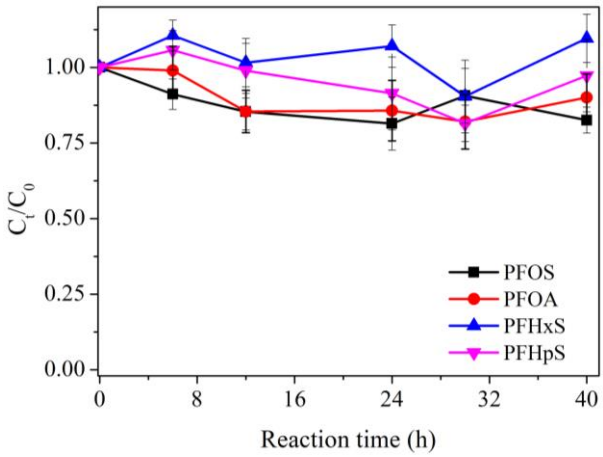

Fig. A2 Sorption of PFOS, PFOA, PFHxS, and PFHpS in still bottom I by Ti_4O_7 electrode. Current density = 0 mA·cm^{-2}. Error bars mean standard deviation of replicates.

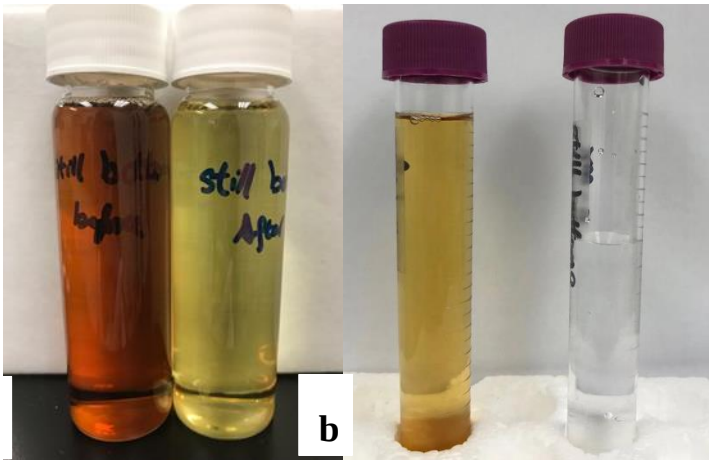

Fig. A3 The color of still bottom I (a) and II (b)during electrochemical oxidation. Left and right are before and after treatment.

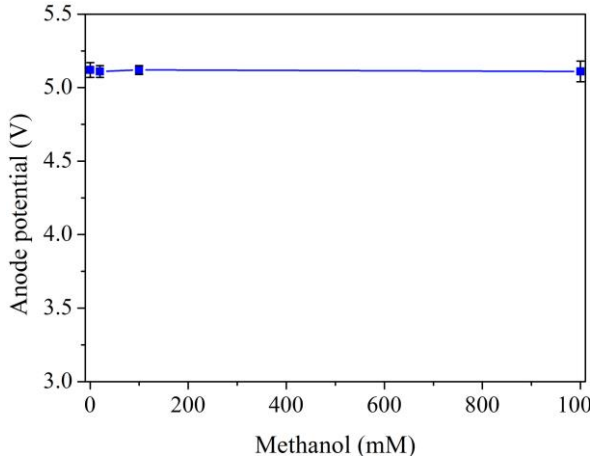

Fig. A4 The anodic potential on Ti_4O_7 in Na_2SO_4 solution with methanol spiked. during the oxidation of Cl^-. $[Cl^-]_0$= 1 mM, $[Na_2SO_4]$= 100 mM, $[Methanol]_0$= 20-1000 mM, current density = 10 $mA \cdot cm^{-2}$. Error bars mean standard deviation of replicates.

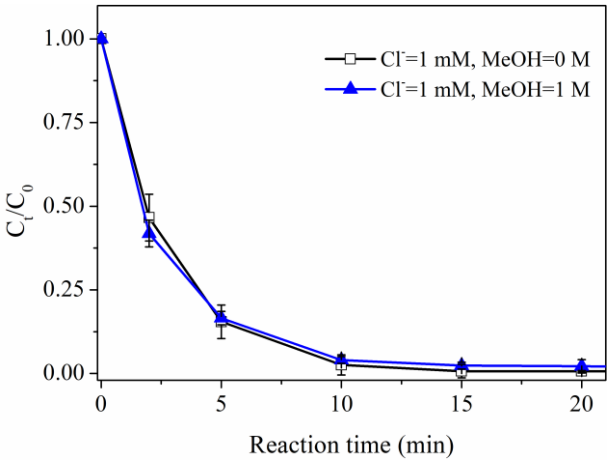

Fig. A5 Effect of methanol on degradtiong of PFOS during the oxidation of Cl^-. [Na_2SO_4]= 100 mM, current density = 10 mA·cm^{-2}. Error bars mean standard deviation of replicates.

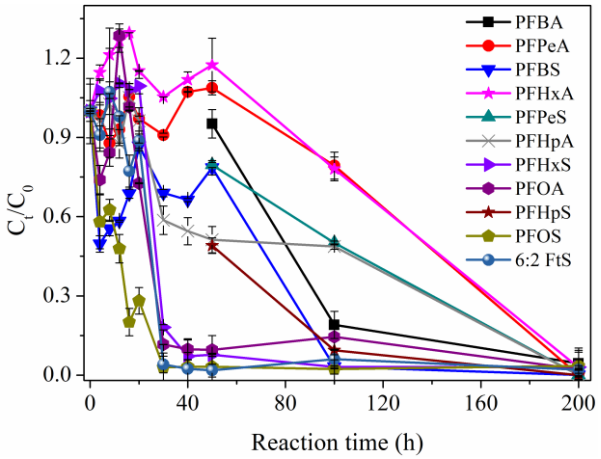

Fig. A6 Degradation of PFASs in still bottom II during electrochemical oxidation treatment on Ti_4O_7 electrode with time. Current density = 10 mA·cm^{-2}, reaction time = 200 h. Error bars mean standard deviation of replicates.

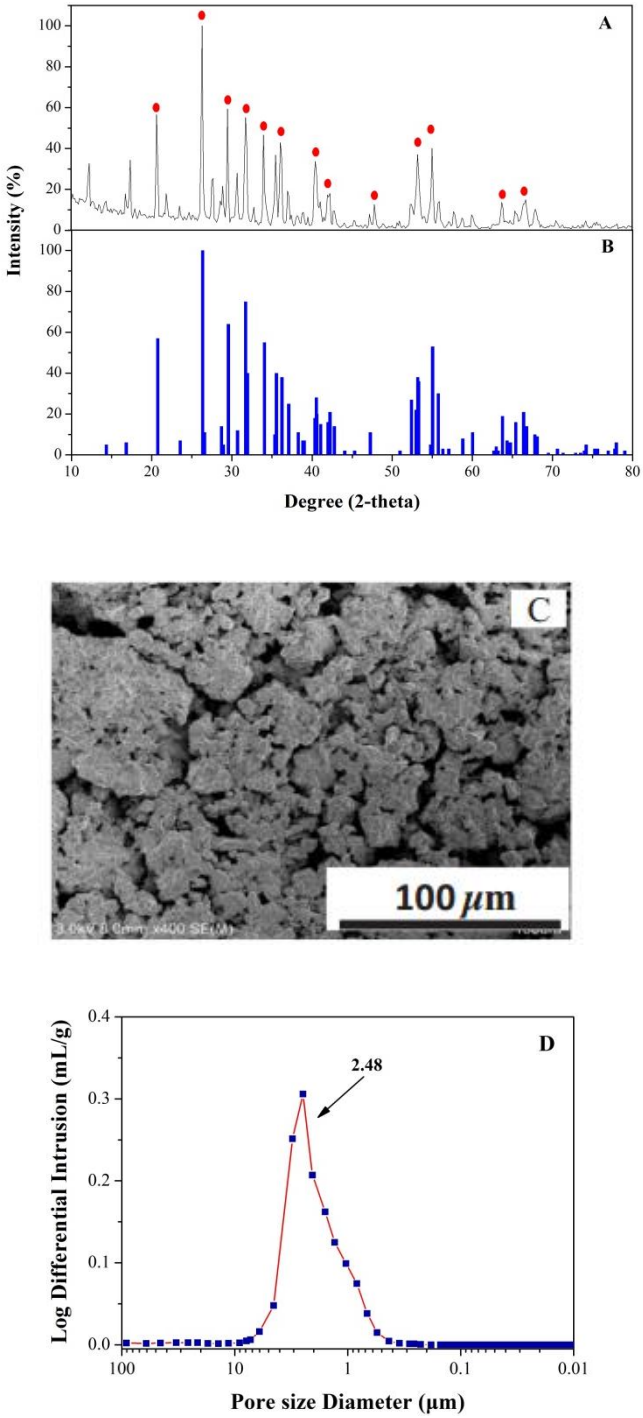

Fig. A7 XRD data of Magnéli phase Ti_4O_7 electrode material (A) and reference Ti_4O_7 powder (B); SEM image of Ti_4O_7 electrode material (C); Result of mercury intrusion analysis of pore size distribution (D)

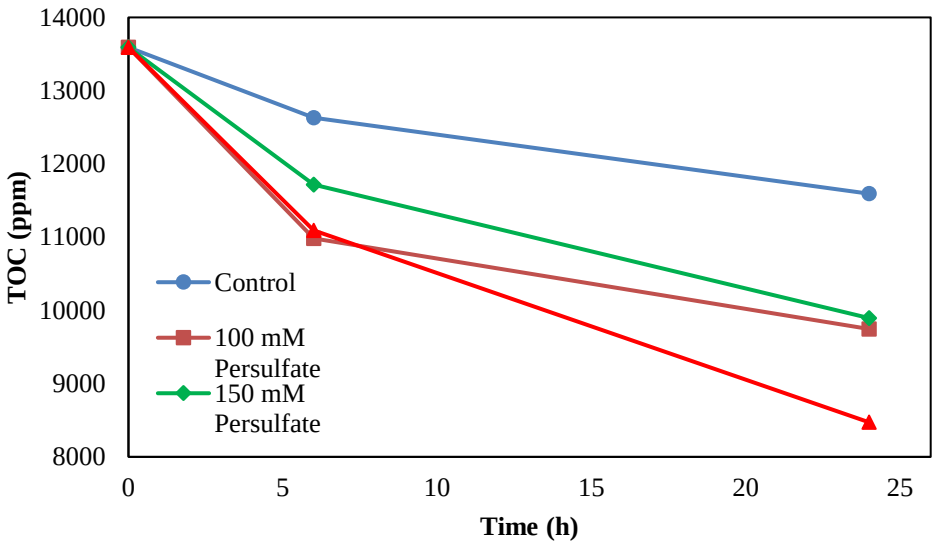

Fig. A8 Degradation of TOC in still bottoms I over time with different concentrations of persulfate at 60 ºC

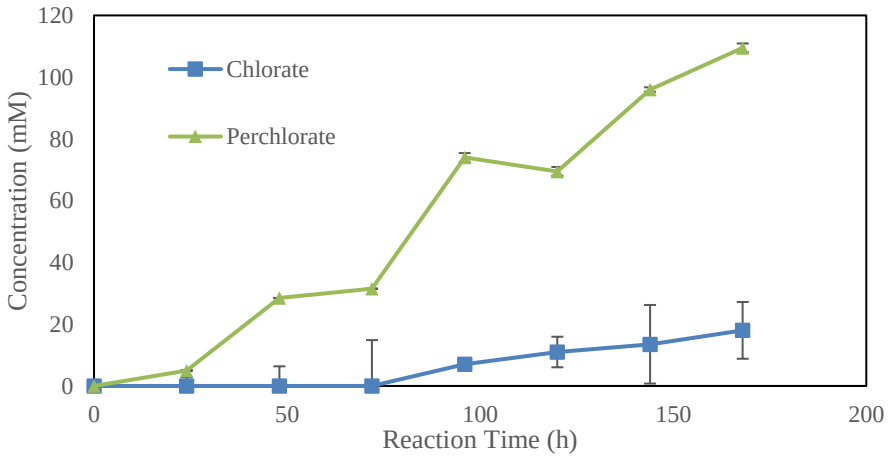

Fig. A9 Formation of ClO_3^- and ClO_4^- during the EO treatment of the still bottom I sample that had been subjected to 200-mM persulfate treatment for 24 hrs. Current density = 10 mA·cm-2.

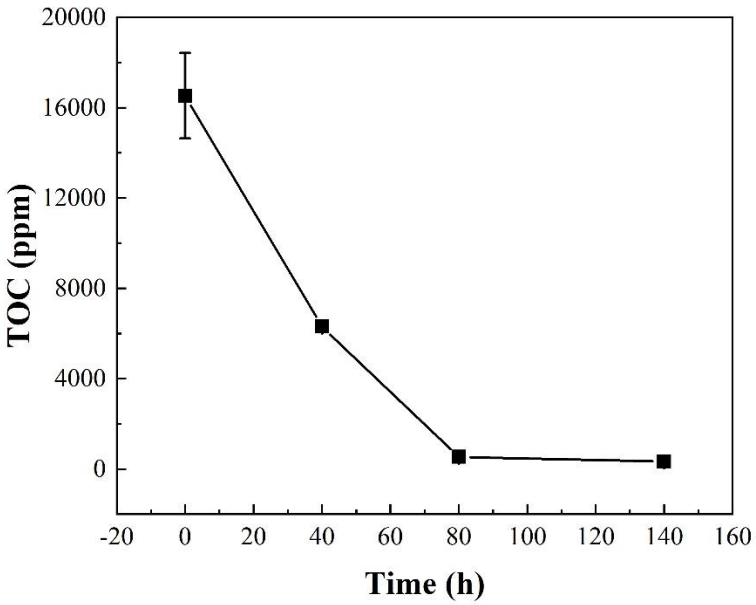

Fig. A10 TOC removal in still bottom III during EO treatment on Ti_4O_7 electrode with time. Current density = 10 $mA \cdot cm^{-2}$. Error bars mean standard deviation of replicates.